IEEE Access
Multidisciplinary ⋮ Rapid Review ⋮ Open Access Journal

Received March 8, 2022, accepted March 25, 2022, date of publication March 28, 2022, date of current version April 7, 2022.

Digital Object Identifier 10.1109/ACCESS.2022.3162904

Hierarchical Multi-Objective Optimization of Automobile Seat Frame Based on Grey Fuzzy Logic System

WEI WANG[1], XIAOJUN LAN[2], AND JIANGQI LONG[1]

[1]College of Mechanical and Electrical Engineering, Wenzhou University, Ouhai District, Wenzhou, Zhejiang 325035, China
[2]Wenzhou Dongqi Auto Parts Manufacturing Company Ltd., Wenzhou, Zhejiang 325700, China

Corresponding author: Jiangqi Long (longjiangqi@163.com)

This work was supported in part by the Wenzhou Major Science and Technology Innovation Project of China under Grant ZG2021028, and in part by the National Natural Science Foundation of China under Grant 51475336.

ABSTRACT In development of the automobile industry, lightweight and safety performance are contradictory, yet they are of great significance.The optimization process of auto parts is a high-dimensional optimization problem which has a variety of regulations limits and safety tests at the same time. In order to address this issue, hierarchical multi-objective optimization of a passenger car seat frame is carried out in this research. Different from previous researches, in this paper, all car seat frame parts are listed as the optimization objects and are given different optimized attributes. Meanwhile, in order to achieve the goal of effectively reducing the sample sizes of the design of experiments, hierarchical optimization is proposed, and the optimization process is divided into three stages. In each stage, components with different optimized attributes are introduced into various safety tests and then conducting design of experiments. On the other hand, through adopting the grey fuzzy logic system to assign the appropriate optimized grade, the optimization process is simplified and the errors caused by the manual selection or unified optimization levels are avoided. The proposed method is considered to be an universal approach to solve the lightweight optimization of the auto parts. Design parameters of the car seat frame before and after the hierarchical multi-objective optimization are compared, it illustrated that total mass and material cost of the seat frame are reduced by 2.3kg (28.5%) and ¥13.8 (32.4%) respectively. Moreover, various comparisons are carried out to verify the validity of the optimization method proposed in this paper. In conclusion, the proposed method is quite promising yet with less sample points associated, is an effective mean to solve the multi-objective optimization problems of automobile component.

INDEX TERMS Automobile seat frame lightweight, hierarchical multi-objective optimization, adaptive design of experiments, grey fuzzy logic system.

I. INTRODUCTION

Lightweight of the auto components has many benefits, studies have shown that mass reduction in automobiles may effectively improve fuel economy, ensure better dynamic handling performance and assist the protection of environment [1]. Therefore, tremendous efforts have been made in the development of automotive lightweight [2]–[6]. The employing of new materials [7], [8] and topological optimization [9]–[11] are the most commonly used methods which can conduct the preliminary optimization of the components. However, deeper optimizations are needed to cope with increasingly stringent emissions regulations. A large proportion of relevant studies focused on the issues associated to body-in-white (BIW), car doors, automotive chassis, etc. [12]–[15]. Automobile seats, accounting for 3-5% of the total vehicle mass [16], are the direct contact medium between vehicles and passengers. Though the seat assemblies affect the comfort and the safety of drivers strongly [17], [18], it has been less noticed by researchers in previous studies. On the other hand, the metal frame is the bearing and the heaviest component of the automobile seat assembly, offering the greatest

The associate editor coordinating the review of this manuscript and approving it for publication was Yiming Tang.

lightweight potential. However, achieving the lightweight and ensuring the safety performance are not binary. Reckless mass reduction may lead to increasingly broken and accidents. Hence,it is also prone to a unsafe product, although the unreasonable lightweight designs can achieve the purpose of reducing mass in a manner. Generally, lightweight and safety are two contradictions in the design process of automobile seat, yet each metric has its own significance. On account of the opposite relationship of optimization targets, this paper considers the car seat frame optimization as a multi-objective optimization question to achieving a reasonable balance.

Unremitting researches have been carried out in the field of multi-objective optimization of the engineering application and automotive components. Prakash *et al.* introduced Taguchi-grey relational analysis method (TGRA) to the multi-objective optimization of workpiece materials and technological parameters, then they determined optimal parameters for improving the surface smoothness and material removal rate in the rock dust reinforced aluminum turning process [19]. Wang and Cai proposed a hybrid method that combines modified non-dominated sorting genetic algorithm (MNSGA-II) and grey relational analysis (GRA), after which they improved the static and dynamic performance of BIW with a small increase on total body mass [20]. To reduce the total mass of BIW while maintaining other mechanical properties, Xiong *et al.* took the side structure of the BIW as research object and then determined the optimal thickness-material combination of the optimized parts based on GRA and principal component analysis (PCA) [21]. By combining GRA with the Analytic Hierarchy Process (AHP), Pu and Ma solved the problem of selecting lightweight materials for BIW and verified the feasibility of this method through an example [22]. Meanwhile, Xiong and Zhang built optimization models of the static and dynamic stiffness along with the front and side crushability for the body in white (BIW). Then, they adopted radial basis function (RBF), multi-objective particle swarm optimization algorithm (MOPSO), and modified grey correlation analysis (MGRA) to construct a metamodel, which solved the optimization process, and obtained the optimal compromise scheme, respectively [23]. To sum up, in order to solve the multi-objective optimization problems which is characterized by many design variables and design levels, two approaches are frequently adopted. The first approach is AOW that can obtain a pareto front by building surrogate models based on sample points and then introduce optimization algorithms to perform the global optimization. The advantage of AOW is that it can theoretically acquire a pareto front which contains the global optimal solution of the optimization problems. Disadvantages of AOW is that the fitting accuracy of surrogate models must be supported by selection experience and the number of sample points, in addition, AOW should be matched with suitable approximation techniques, sampling methods, and optimization algorithms [24]. This makes the modeling and the solving process of AOW relatively complicated. The second approach is MW that adopts multi-criteria decision-making method to select the optimal scheme in the sample points directly. The advantage of MW is that it features a simple process and requires fewer sample points. Disadvantages of MW is that since the limits of the sample sizes and purposeless range of DoEs, the optimal compromise scheme has a certain design margin.

As for the lightweight optimization of the auto seat frame, on account of the various safety test conditions and the regulatory requirements of much local performance, seat frame multi-objective optimization is a high-dimensional, complex, nonlinear work with many design variables, design levels and safety tests. Under such circumstances, it means large sample size and the inefficient fitting process while adopting AOW. Meanwhile,, design of experiments (DoEs) are necessary and important when employing whether AOW or MW. To be exact, DoEs affects the fitting accuracy of the surrogate model when AOW is used, and also determines the remaining design margin of the optimal compromise solution when MW is used. However, rare studies focus on improving the covering efficiency of DoEs within limited sample points. Therefore, adaptive DoEs is proposed in this paper to solve the problem

Previous seat optimization researches tend to list some components with high lightweight potential as optimization object or treated the mirrored components as a object to be optimized. Meanwhile, for the purpose of reducing the sample sizes and simplifying the optimization process [25], [26], some studies only focused on the thickness or materials of components to simplify the optimization problems [27], [28]. Besides, single range of DoEs and one certain safety optimization test are also frequently employed. However, the above optimization method has several disadvantages. Firstly, the universal applicability of the optimal compromise scheme in a single safety test has not been demonstrated in other tests. In fact, the optimal thickness-material compromise solution based on a single test may even result in a failed scheme that cannot meet the experimental requirements of other tests. Therefore, the possible weak parts in the proposed optimization process should be strengthened. Secondly, the loading conditions of all seat frame parts are quite different so that their strength contributions in different safety tests vary even for symmetrically designed parts. Therefore, mirrored designed components should be treated as different optimization objects and optimized separately. Thirdly, the same design range of DoEs is not suitable for the parts with different optimization demands. it is obviously that employing the same design range ignores the differences in strength contributions. Hence, ranges of DoEs should be determined based on respective characteristics.

This paper treats all parts as optimization objects and employs adaptive DoEs to multi-objective optimize a automobile seat frame hierarchically. The first innovation of this study is that design variable parameters including discrete material and continuous thickness are employed. Besides, all seat frame parts are regarded as optimization objects separately, and the safety performances are validated under all safety tests. The second innovation focus on promoting the filling efficiency, grey fuzzy logic system (GFLS) who

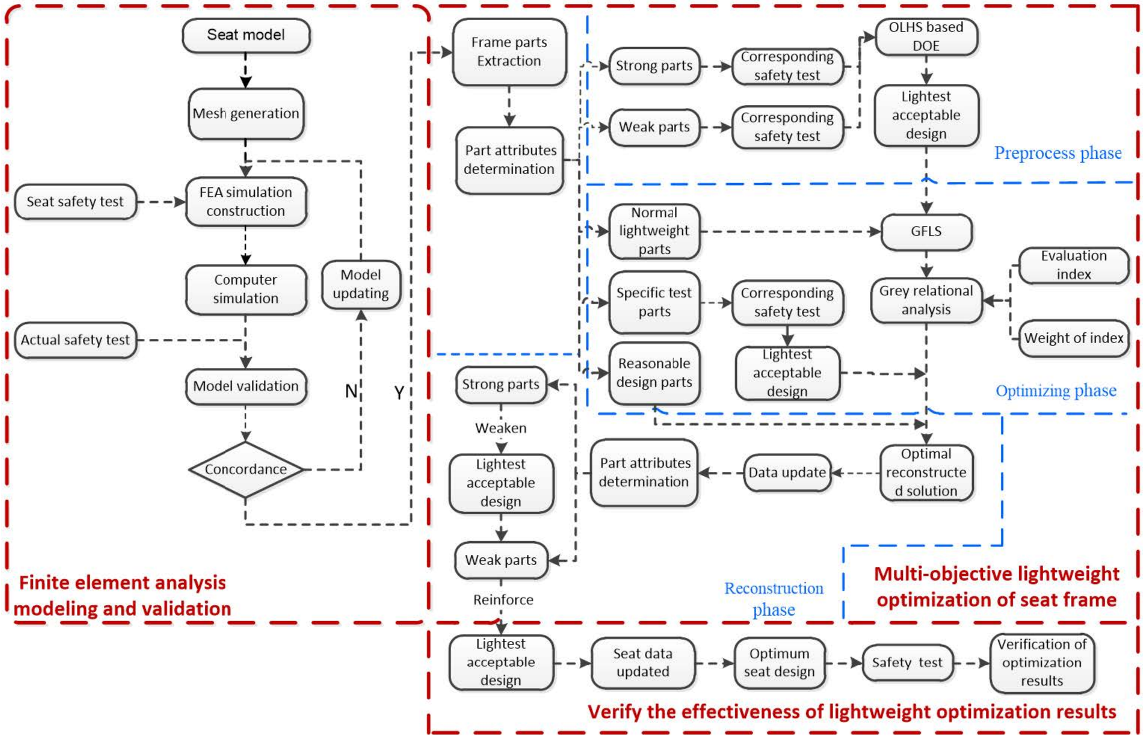

FIGURE 1. Flowchart of automobile seat frame hierarchical multi-objective optimization.

combines GRA and fuzzy logic system (FLS) to adaptively conduct the DoEs are proposed. In the GFLS, GRA conducts the dimensionless processing on the initial sequences of the mass and energy absorption firstly. Since the strain index of a component represents the extent of the damage to the parts and normally the strain index changes between 0 to 1, the sequence of strain indices are not imported to GRA. Then, FLS calculates the specific optimized grade through identifying the calculated grey relation coefficient (GRC) of the mass-energy absorption sequences and the unprocessed strain index sequence.The concepts of optimized attribute and optimized grade are proposed. The specific optimized grade determines the DoE range of continuous thickness variables and discrete material parameters of a single part. The optimized attributes are acquired through estimating energy absorption and strain indices of the frame parts under all safety tests, determining the specific optimization means of frame parts. Nevertheless, adopting all frame components and multiple safety tests will lead to the growing in sampling size and the sampling frequency eventually. As a solution, hierarchical multi-objective optimization is employed to consider the purpose of the DoEs in different phases so that more sample points are distributed around the theoretical global optimal compromise. Hierarchical multi-objective optimization has been used in the fields like post-earthquake medical evacuation, flight allocation and design of electric vehicles [29]–[31]. Hierarchical multi-objective seat frame optimization has several features and advantages:

- Different phases have respective optimization objectives and the components to be optimized. Compared with carrying out DoEs directly at the same time, the number of design variables for each DoE is reduced and a large number of invalid sample points are avoided.
- In each phase of the hierarchical optimization, the feasibility of the optimization schemes is verified. The applicability of the final optimization scheme in all safety test conditions is ensured.
- the optimization objectives of each phase are clearly defined, so as are the optimization attributes. As a result, the hierarchical optimization process adopting GFLS can be used to optimize other auto parts which featured with high-dimensional and multi-objective directly.

The SFMOO is divided into three phases, namely, the preprocessing phase, the optimizing phase and the reconstruction phase. FIGURE 1 shows the detailed optimization flowchart. Firstly, in the preprocessing phase, the parts whose optimized attributes are specific test part, strong part, and weak part are optimized in the safety test with largest strain index. The lightest qualified scheme is adopted. Secondly, in the optimizing phase, GRA is used to determining the optimal compromises of local safety tests. Then, the GFLS identifies the mass, energy absorption, and strain indices of the normal lightweight part, the optimized strong and weak parts, after that GFLS can export the specific optimized grades matching with load conditions of components and conduct adaptive DoE. Thirdly, in the reconstruction phase, all optimal designs of global safety tests are updated to the reconstructed frame model, performance evaluations under all safety tests are carried out subsequently. Based on the strain indices of each component in all safety tests, the strong and weak parts are partially modified.

The rest of this paper is organized as follows. Section 2 introduces typical seat safety tests and establishes the seat finite element model. The accuracy of the established model is validated by comparing the variation of key measuring indicators of each test in the actual experiment test and computer simulation. Section 3 systematically introduces the mathematical model of SFMOO and the related methodologies of GRA and GFLS, followed by the creation of the Mamdani-based GFLS. in Section 4, the detailed definitions of optimized attribute, optimized grade and relevant optimization strategy are introduced. Section 5 describes each step of the proposed method and records the data. In Section 6, the optimal compromise scheme is presented and two comparisons are conducted for validating the effectiveness of the proposed method. Finally, Section 7 summarizes the article.

II. SAFETY PERFORMANCE TESTS, FINITE ELEMENT MODELING AND VALIDATION

A. SAFETY PERFORMANCE TESTS

Passenger car seat safety performance tests include dynamic and static conditions. The dynamic conditions include forward collision (FC), rear collision (RC), trunk collision (TC), etc. while static conditions include seatbelt anchor test (SAT), headrest static strength test (HSST), seat backrest strength test (SBST), antisubmarine pan test (APT), front ultimate load (ULF), rear ultimate load (ULR), child protection test (CPT) and low speed rear neck protection test (whiplash test), etc. Specially, seat dynamic crash tests require dummies, in this paper, the 50-percentile male dummy is used. As shown in FIGURE 2, 50-percentile male dummy forward collision (50FC), 50-percentile male dummy rear collision (50RC), SAT, SBST, HSST, APT, ULF and ULR are taken as the seat safety tests. Detailed procedures and standards of above safety tests are mentioned in [25]. It is necessary to point out that 50FC and 50RC are global dynamic tests involved in investigating the overall seat performance under the condition that the vehicle is impacted from the front and rear directions respectively. SAT, HSST, SBST, APT, ULF and ULR are local static tests related to inspecting partial seat performance. Moreover, APT and ULR investigate the bearing capacity of a single seat frame, often lead to the destruction of local seat frame parts. Meanwhile, FEA in this paper does not involve the situation after material fracture. Therefore, the curves of measurement points obtained in APT and ULR may both have certain differences among actual experiments and simulations. Moreover, the displacement of the measurement continues to change when failure occurs in the simulation. Therefore, the test processes are stopped in the actual test process when failure happened.

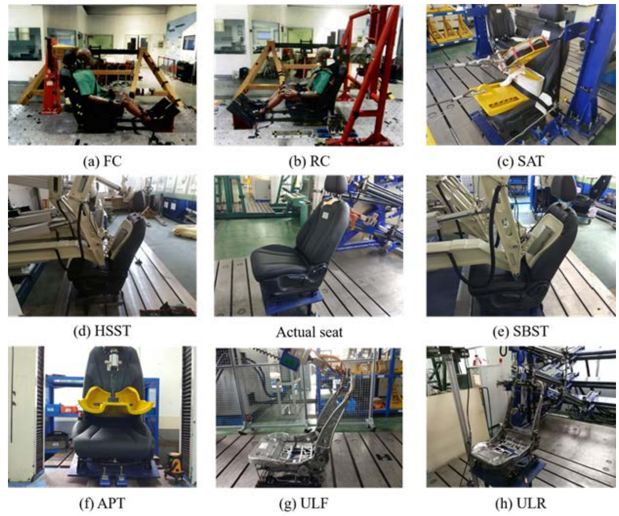

FIGURE 2. Actual seat and introduced seat experimental tests.

B. MODELING AND ACCURACY VERIFICATION

After years of development, computer aided engineering (CAE) has been developed into an effective measure in the field of engineering optimization. Based on the seat model shown in FIGURE 2, the pre-processing software Hypermesh is adopted to construct the mesh model and the LS DYNA is employed to set up the safety simulation tests. The computer simulation models are listed in FIGURE 3.

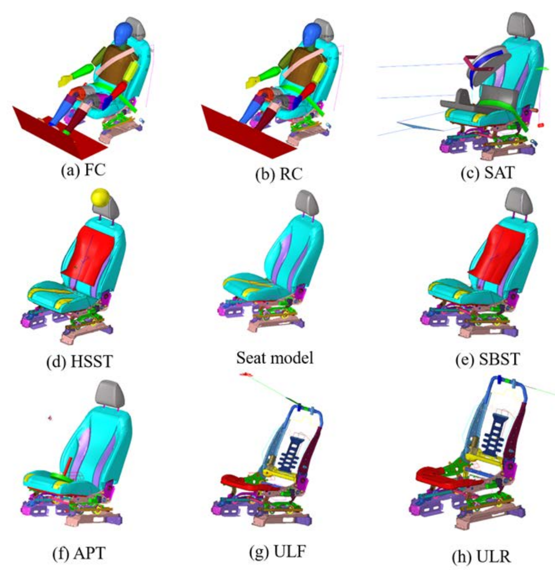

FIGURE 3. Seat model and computer simulation safety tests.

Although computer simulation can greatly reduce test cost [32]–[35], an accurate FEA model is a precondition for reliable simulation results. To validate the model accuracy of APT, ULF and UIR, HSST, SAT, 50FC and 50RC, and SBST. FIGURE 4 shows the performance measurements involving points A, B, C, E, H, and angle Db for each safety test respectively. Specifically, A is the midpoint of the front tube

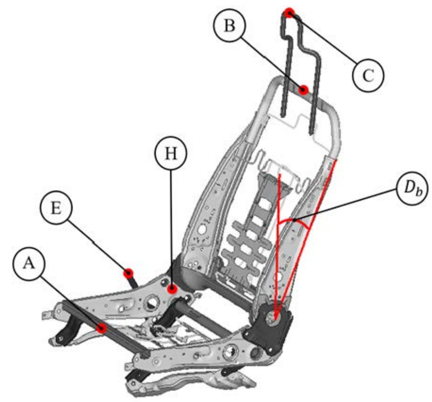

FIGURE 4. The performance measurement points of all tests.

under the seat frame pan, B is the midpoint of the backrest upper circular tube, C is the midpoint of the headrest tube, E is the installation position of the seat belt buckle and H is anchor point inside the dummy, angle Db is the included angle between side backrest and the vertical direction. The variation trends, peak values of measurement indices obtained in simulations and actual tests are the judgment criteria in the model accuracy validation.

Based on these comparison result shown in FIGURE 5, computer simulation result in ULF, HSST, SAT, 50FC, 50RC, and SBST are basically consistent with the experimental test results. Simulation results of APT and ULR have some acceptable deviation from the actual test due to the fact that some parts are damaged. In summary, the simulation model and safety test established in this paper have high accuracy and can be used for subsequent SFMOO.

III. METHODOLOGY

A. MATHEMATICAL MODEL FOR SEAT FRAME MULTI-OBJECTIVE OPTIMIZATION

In this paper, continuous thickness parameters and discrete material types are taken as design variables. The alternative materials are assigned numbers $M_i, i \in \{1, 2 \ldots, q\}$ according to their yield strength. Mathematical model of M_i has a form, can be expressed as follows [21]:

$$\begin{pmatrix} \rho_i \\ E_i \\ P_i \\ \vdots \end{pmatrix} = \begin{pmatrix} f_\rho (M_i) \\ f_E (M_i) \\ f_P (M_i) \\ \vdots \end{pmatrix} \tag{1}$$

where, ρ_i, E_i, P_i is material density, elastic modulus and raw material price, q is the number of alternative materials, $f_\rho (M_i)$ is the mathematical expression between ρ_i and M_i, $f_E (M_i)$ is the mathematical expression between E_i and M_i, and $f_P (M_i)$ is the mathematical expression between P_i and M_i.

Meanwhile, the mathematical model of SFMOO can be expressed as follow [36]:

$$\begin{aligned} Minmize\ W &= W (T_i, \rho_i) \\ &= \sum\nolimits_{i=1}^{z} A_i T_i \rho_i = W \left(T_i, f_\rho (M_i)\right) \\ &= W (T_i, M_i), \\ &\qquad i = 1, 2, \cdots, z \end{aligned} \tag{2}$$

$$\begin{aligned} Minmize\ C &= C (T_i, \rho_i, P_i) \\ &= \sum\nolimits_{i=1}^{z} A_i T_i \rho_i P_i = C \left(T_i, f_\rho (M_i)\right) \\ &= C (T_i, M_i), \\ &\qquad i = 1, 2, \cdots, z \end{aligned} \tag{3}$$

$$\begin{aligned} Minmize\ P (T, M) & \\ &= (minP_1 (T_i, M_i), minP_2 (T_i, M_i), \cdots, \\ &\qquad minP_s (T_i, M_i)), \\ &\qquad i = 1, 2, \cdots, z \end{aligned} \tag{4}$$

$$s.t. \begin{cases} g_j (T_i, M_i) \leq 0, \quad i = 1, 2, \cdots, z;\ j = 1, 2, \cdots, b \\ T_i^L \leq T_i \leq T_i^U, \quad i = 1, 2, \cdots, z \\ M_i \in \{1, 2, \cdots, q\}, \quad i = 1, 2, \cdots, z \end{cases} \tag{5}$$

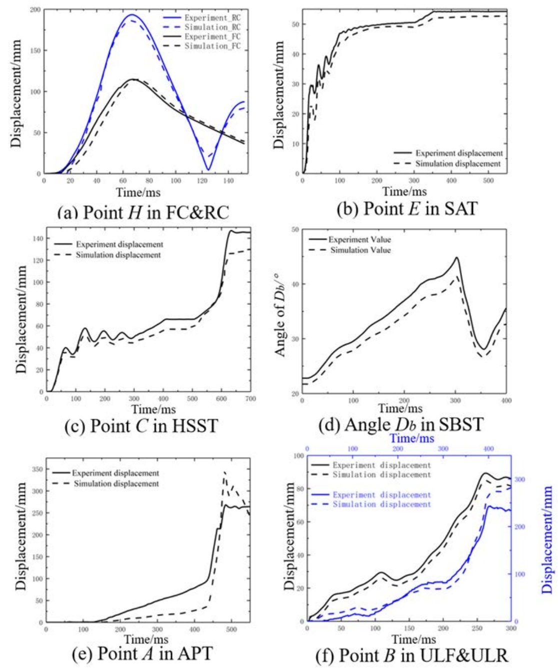

FIGURE 5. Changes of measurement indicators in seat simulations and actual experimental tests.

where, T_i and A_i are thickness and area of the part P_i respectively, T_i^L and T_i^U are lower and upper design bounds of T_i, z represents the amount of frame parts, W and $W (T_i, M_i)$ is the total mass of car seat frame, C and $C (T_i, M_i)$ is the material cost of car seat frame, $P (T, M)$ is the seat performance index vector which contains lightweight index, comfort index or safety index, $P_s (T_i, M_i)$ represents the sth seat performance index, $g_j (T_i, M_i)$ represents the jth constraint of seat performance index, b is the number of constraints.

The above mathematical model expresses the SFMOO whose characteristic includes high dimension and strong nonlinearity. In SFMOO, each thickness design parameter is continuous while the material parameter is discrete. Due to the large number of design variables, design levels, optimization tests and long calculation time, this paper combines GRA and fuzzy logic system (FLS) to obtain the optimal thickness-material scheme of reasonably design frame parts in each safety tests.

B. STRAIN INDEX AND ENERGY ABSORPTION

This paper introduces strain index to determine the damage to parts, calculation equation of strain index is listed as follows:

$$SI_{P_i} = \frac{S_{p_i}}{E_{p_i}} \tag{6}$$

where, P_i is the parts number of components, SI_{P_i} is the strain index of the part P_i, S_{p_i} represents effective plastic strain of the part P_i and E_{p_i} represents elongation at the fracture of corresponding material. In reality, parts will fracture when SI_{P_i} is 1. Nonetheless, considering that linkage brackets have the great influence on passenger comfort, the design safety threshold of linkage brackets is set as "0.7". Meanwhile, to ensure that remaining seat frame parts have a certain design margin, a safety threshold "0.95"is given in the subsequent optimization. In other words, linkage brackets and the remaining seat frame parts will be deemed as failure when SI_{P_i} is greater than 0.7 and 0.95 respectively. On the other hand, the safety threshold in this paper is not only employed in the failure judgment of frame components but also in safety tests. Furthermore, the values of force and torque stipulated by corresponding test criteria are increased to 1.2 times both in actual test and simulation, so as to ensure the reliability of the final design scheme in actual use.

Energy absorption is the sum of energy absorbed by the structure during the whole deformation process, and its expression is as follows [37]. The differences of energy absorption determine the importance of each component in the same seat structure during different safety tests.

$$E_A(d) = \int_0^d F(x)dx \tag{7}$$

where, $F(x)$ is the instantaneous impact force that is a function of impact distance normally, d is the impact distance. In this paper, energy absorption is employed in determining the optimized attribute and specific optimized grade of a single component. Furthermore, energy absorption is introduced along with strain indices to determine the optimized attribute of a single part. Also, energy absorption, strain indices and mass are imported into GFLS to determine the specific optimized attribute of a single reasonably designed part.

C. GREY RELATIONAL ANALYSIS

The grey theory, first proposed by Deng [38], [39], is the tool to study grey systems. Grey relational analysis (GRA) has the characteristics of flexible and strong compatibility, is an effective method in studying multi-objective questions with complex relationships among variables. The basic steps of GRA are listed as follows [40].

When the optimum of an original sequence is "large expectation", the original sequence is normalized as follows:

$$x_i^*(t) = \frac{Max_t x_i(t) - x_i(t)}{Max_t x_i(t) - Min_t x_i(t)} \tag{8}$$

When the optimum of an original sequence is "small expectation", the original sequence is normalized as follows:

$$x_i^*(t) = \frac{x_i(t) - Min_t x_i(t)}{Max_t x_i(t) - Min_t x_i(t)} \tag{9}$$

When the optimum of an original sequence is a target value, the original sequence is normalized as follows:

$$x_i^*(t) = 1 - \frac{|x_i(t) - Tar|}{MAX\{Max_t x_i(t) - B, A - Min_t x_i(t)\}} \tag{10}$$

where $x_i^*(t)$ is the normalized sequence, $x_i(t)$ is the ith value in tth original sequence, $Max_t x_i(t)$ is the maximum value in tth original sequence, $Min_t x_i(t)$ is the minimum value in tth original sequence, Tar represents the target value. $i = 1, 2, 3, \ldots, m_1, t = 1, 2, 3, \ldots, m_2$, m_1 represents the number of values in a sequence, m_2 represents the number of sequences.

All evaluation indices in this paper have the feature of "small expectation". Meanwhile, the reference sequence in this paper is defined as 1, the closer the normalized sequence is to the reference sequence, the better the performance is.

Grey relation coefficient (GRC) can determine the correlation between the reference sequence and the normalized sequences. The calculation equation of GRC is as follows:

$$\gamma\left(x_r^*(t), x_i^*(t)\right) = \frac{\Delta_{min} + \mu\Delta_{max}}{\Delta_{ri}(t) + \mu\Delta_{max}} \tag{11}$$

where $\gamma\left(x_r^*(t), x_i^*(t)\right)$ is grey relation coefficient (GRC), μ is the different coefficient whose value normally is set as 0.5. $\Delta_{ri}(t)$ is the distance between $x_i^*(t)$ and the reference matrix $x_r^*(t)$, Δ_{min} is the minimum value in $\Delta_{ri}(t)$, Δ_{max} is the maximum value in $\Delta_{ri}(t)$. Calculation equations of $\Delta_{ri}(t)$, Δ_{min}, Δ_{max} are listed as follows respectively:

$$\Delta_{ri}(t) = \left|x_r^*(t) - x_i^*(t)\right| \tag{12}$$

$$\Delta_{min} = \underbrace{\min}_{\forall i}\underbrace{\min}_{\forall t}\Delta_{ri}(t) \tag{13}$$

$$\Delta_{max} = \underbrace{\min}_{\forall i}\underbrace{\min}_{\forall t}\Delta_{ri}(t) \tag{14}$$

The following formula is adopted to calculate grey relational degree (GRG):

$$\varphi\left(x_r^*, x_i^*\right) = \sum\nolimits_{t=1}^{n} w_t\gamma\left(x_r^*(t), x_i^*(t)\right) \tag{15}$$

where w_t is the weight of tth objective, n is the number of optimization objectives.

D. ADAPTIVE DESIGN OF EXPERIMENT

The uniform range of DoEs does not take differences in strength contributions of each part into account. Therefore, employing adaptive DoE identifies the design variables and determine the design level according to the contribution of

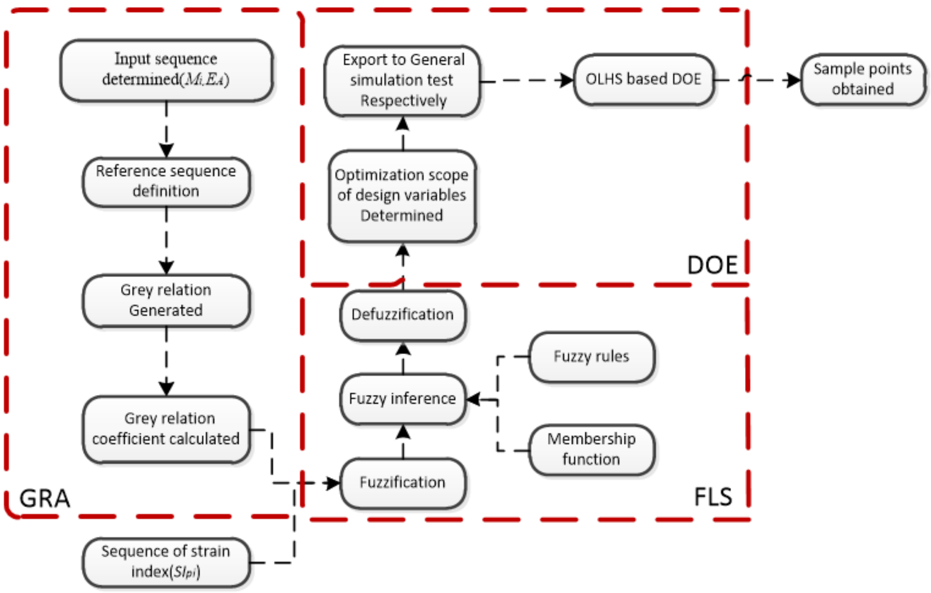

FIGURE 6. **Flowchart of grey fuzzy logic system.**

strength and energy absorption in each safety test. To be exact, energy absorption, strain index and mass of parts are imported to GFLS, which automatically generates sample points according to the component characteristics in the optimization phase. Different from the traditional fuzzy logic system (FLS), GFLS can dimensionless process the initial data sequences so that the GFLS can be applied to the optimization process of a variety of automobile parts.

As shown in FIGURE 6, GRA and standard Mamdani fuzzy logic system are combined as a GFLS. In this paper, to obtain the optimized grades of components that are suitable for different "energy absorption-mass-plastic strain" conditions. The GRC of parts energy absorption, mass obtained by Equation 10 along with actual strain index of frame parts are imported into the FLS.

Mamdani firstly proposed fuzzy control based on the fuzzy theory originally studied by Zadeh [41]–[43]. Fuzzy logic system is an effective method to deal with questions having an imprecise and undefined boundary [44]. Another advantage of FLS is that expert knowledge and engineer experience is important references for fuzzy logic control [45]–[47]. Meanwhile, relevant recent researches shows that the fuzzy set theory has wide applications in the field of multi-criteria decision making (MCDM), linear programming (LP), control of robot, Shortest Path planning and dealing with uncertainty [51]–[53]. Furthermore, FLS may exports continuous control signal based on the discrete membership functions and fuzzy rules. The general process of a FLS includes fuzzification, fuzzy logic inference and defuzzification [54], [55].

In the process of fuzzification, membership functions are applied to transform the exact values to vague languages. This paper applies the triangular membership functions, of which the advantages is simple structure and high calculation efficiency. Calculation equation of triangular membership function is listed as Equation 16.

$$f(x, a, b, c) = \begin{cases} 0, & x < a \\ \dfrac{x-a}{b-a}, & a \le x \le b \\ \dfrac{c-x}{c-b}, & b < x \le c \\ 0, & c < x \end{cases} \tag{16}$$

Detailed parameters and polylines of fuzzy inputs and output are shown in FIGURE 7. The fuzzy inputs involve the actual strain indices and the GRC of energy absorption and mass. Membership functions of the input actual strain index have five language levels, and membership functions of the input GRC of energy absorption and mass have three language levels. As for output variable, membership function of optimized grade defines six grey fuzzy reasoning levels corresponding to the basic optimized grades employed frequently in engineering optimization.

Fuzzy inference is another key process in GFLS, it maps fuzzy input set to exact output set according to the fuzzy rules. Takagi and Sugen first comprehensively proposed the fuzzy rules of "IF-Then" form [56], the general type of "IF-Then" is shown in Equation 17. "IF-THEN" rules can model human knowledge and reasoning processes without precise quantitative analysis [57]. The developed fuzzy inference systems combined with "IF-THEN" rules have been widely used in control [58], prediction [59] and reasoning [60].

$$Rule: if\ "condition"then"restriction"$$
$$Rule1: if\ "x_1\ is\ A_1\ and\ x_2\ is\ B_1\ and\ x_3\ is\ C_1"then"y\ is\ D_1"$$

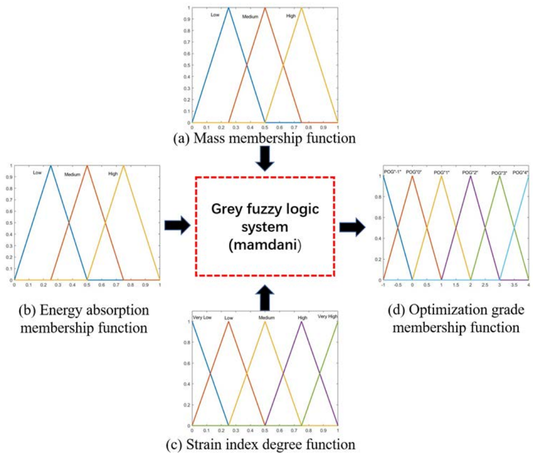

FIGURE 7. Membership functions of input and output in GFLS.

$$\begin{aligned} &Rule2: if\,"x_1\, is\, A_2\, and\, x_2\, is\, B_2\, and\, x_3\, is\, C_2"then"y\, is\, D_2" \\ &\qquad\qquad \cdots\cdots\cdots \\ &Rulen: if\,"x_1\, is\, A_n\, and\, x_2\, is\, B_n\, and\, x_3\, is\, C_n"then"y\, is\, D_n" \end{aligned} \tag{17}$$

where, x_1, x_2, x_3 are the input, y is the output, they are all fuzzy language values. $A_i, B_i, C_i, D_i(i = 1, 2, \cdots, n)$ is the fuzzy subset designated by x_1, x_2, x_3 on domain X_1, X, X_3 on the basis of relevant membership function $\mu A_i, \mu B_i, \mu C_i, \mu D_i(i = 1, 2, \cdots, n)$.

According to the parameter information of membership functions and input variables, $45(5^1 \times 3^2)$ fuzzy rules are defined for fuzzy inference. Equation 18 describes the ''max-min'' operation that is adopted to calculate the fuzzy output $\mu F_i(y_i)$ of membership functions:

$$\begin{aligned} \mu F_i(y_i) = &(\mu A_1(x_1) \wedge \mu B_1(x_2) \wedge \mu C_1(x_3)) \\ &\vee (\mu A_2(x_1) \wedge \mu B_2(x_2) \wedge \mu C_2(x_3)) \\ &\vee (\mu A_n(x_1) \wedge \mu B_n(x_2) \wedge \mu C_n(x_3)) \end{aligned} \tag{18}$$

Defuzzification can produce a quantitative result under the conditions that $\mu F_i(y_i)$ has been acquired. Currently, ''center of gravity'' method is frequently used to transform the linguistic outputs to crisp values, specific calculation equation of the crisp value G_i is given as follows:

$$G_i = (\int_s y_i \cdot \mu F_i(y_i)dy)/(\int_s \mu F_i(y_i)dy) \tag{19}$$

Optimized Latin hypercube sampling (OLHS) can reduce the number of simulations on the basis of ensuring the good orthogonality and proportional spacing [61]. OLHS offers good space filling, uniform distribution, less tests and higher exploration precision [62]. Since SFMOO is characterized by many design variables and strong nonlinear qualities, OLHS is employed to enhance the sampling efficiency. The amount and variables of optimized components varies in each optimization phase. Besides, the design purpose in each global optimization test also varies. In this paper, multiple DoEs are performed, to unify the standards for determining the number of sample points, equation 20 is adopted.

$$N = \begin{cases} 5 * (a-1), & preprocess\ phase \\ a^2, & optimizing\ phase \\ 5 * a, & reconstruction\ phase \end{cases} \tag{20}$$

where, N is the number of OLHS sample points in each optimization phase, a is the number of components to be optimized in each phase.

IV. OPTIMIZATION PART, OPTIMIZED GRADE AND OPTIMIZATION STRATEGY

A. OPTIMIZATION PART

To improve the availability of sample points, previous multi-objective automotive optimization studies control the number of components to be optimized and select a part of components as optimization objects for lightweight. As mentioned above, car seat lightweight is a nonlinear work which involves numerous components and safety tests. The importance of a single seat frame part in different safety tests are inconsistent. As shown in FIGURE 8, all seat frame parts are listed as optimization objects in this paper. Table 1 records the discrete alternative materials. Particularly, DC01 and 42CRMO4 are dedicated materials for the seat pan and rear left linkage bracket respectively. Hence, the materials of P15 and P19 will not be replaced in subsequent optimization.

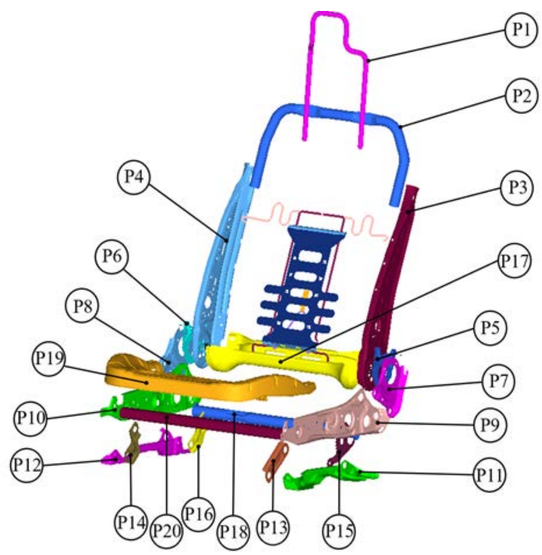

FIGURE 8. Frame model of car seat.

B. OPTIMIZED GRADE

Comprehensive performance contribution of all seat frame components is discrepant. Thus, the optimization levels for different optimized parts should be discrepancy. In previous optimization researches, the optimization level of each part is confined on the basis of initial thickness and material scheme. In order to distinguish the optimization

TABLE 1. Basic information of alternative materials.

No.	Material	Elongation (%)	Cost (¥/kg)
1	DC01	0.27	4.28
2	Q195	0.278	4.49
3	Q235	0.223	4.77
4	SAPH440	0.278	5.02
5	Q345	0.199	5.1
6	QSTE340TM	0.199	5.15
7	QSTE420TM	0.199	5.05
8	B410LA	0.157	5.1
9	S500MC	0.095	5.17
10	S550MC	0.113	5.3
11	QSTE600TM	0.14	5.41
12	SAPH780	0.131	5.48
13	HC700/980DP	0.077	5.56
14	H800LA	0.086	5.7
15	42CRMO4	0.113	9.5

TABLE 2. Details of each optimized grade.

Grade	Optimization objective	Thickness (%)	Material
-2	Thickness, Material	110%~150%, 5 levels	M~M+2, step:1
-1	Thickness, Material	110%~130%, 3 levels	M-2~M, step:1
0		-	
1	Thickness, Material	80%~140%, step:0.1	M-2~M+4, step:1
2	Thickness, Material	70%~130%, step:0.1	M-3~M+3, step:1
3	Thickness, Material	60%~120%, step:0.1	M-4~M+2, step:1
4	Thickness, Material	50%~110%, step:0.1	M-5~M+1, step:1
5	Thickness	50%~90%, 5 levels	-

potential of different parts, as shown in Table 2, eight foundational optimized grades are defined for selection. Nonetheless, the foundational grades are still inaccurate and ambiguous. For determining the specific optimized grade, GFLS is introduced. Meanwhile, the optimized grades "−1", "-2", "5" in Table 2 are only employed in preprocess phase, in which the optimization potential and reinforce demand is greater. Therefore, the distance between each optimization level should be set larger. Introducing optimized grades "−1", "−2", "5" not only reduce the sample size, but also achieve the goal of regulatory requirement quickly. Moreover, the thickness optimized grades of "−2" and "5" each has 5 levels, may export 5 discrete alternate thicknesses based on the initial thickness. Also, the thickness optimized grades of "-1" each has 3 levels, may export 3 discrete alternate thicknesses based on the initial thickness. On the other hand, the material optimized grades of "−2" and "-1" each has 3 levels, may export 3 discrete alternate material based on the initial material. the optimized grades "5" are not optimizing the parameter of materials due to large optimization potential. Furthermore, optimized grades "1", "2", "3", "4" may export all continuous thicknesses with an interval of 0.1 and discrete alternate materials of an interval of 1.

C. OPTIMIZATION STRATEGY

The seat model is imported to each simulation tests for calculation, after which the energy absorption and strain indices of all frame parts are extracted from the calculated results. The optimized attribute of a part is determined by its analytically energy absorption and strain indices. This paper defines five optimized attributes. They are reasonably designed parts, strong parts, weak parts, optimization parts, and specific test working parts:

- Reasonably designed parts: the components are not broken in the seat safety performance tests except in APT and ULR, and the strain indices reach 0.75-0.95 in one or more tests;
- Strong parts: the components whose actual strain indices are less than 0.1 in the seat safety performance tests except in APT and ULR;
- Weak parts: the components are broken in the seat safety performance tests except in APT and ULR;
- Optimization parts: the components whose strain indices reach 0.1-0.75 in one or more seat safety performance tests;
- Specific test parts: the components that only deform under a certain safety performance test and scarcely participate in absorbing energy when other tests are calculated. The special test working part in this paper only refers to the headrest tube in the HSST.

Different part attributes mean different optimization strategies. Here, the relevant optimization test of parts needs to be considered. Then, the corresponding optimization test and optimization strategy of optimization part are defined as follows:

- Reasonably designed parts: Conducting no further lightweight optimization;
- Strong parts: Firstly, strong and weak parts are optimized, OLHS is used to carry out DoEs according to the optimized grade "5" in test with the maximum part strain index, then import the qualified design scheme with minimum total mass into "Optimization part" for further optimization;
- Weak parts: Firstly, OLHS is used to carry out DoEs according to the optimized grade "-1" in test with the maximum part strain index, If the sample points cannot meet the requirements, the optimized grade "-2" will be used later.

Then import qualified design scheme with minimum total mass into "Optimization part" for further optimization;

- Optimization parts: Sample size will be greatly increased if parts are introduced into many seat safety performance tests for DoEs. In addition, the optimal compromises of multiple safety performance tests are not uniform. It must be noted that seat safety tests can be divided into static local tests including APT, HSST, SAT, SBST, ULF, ULR and dynamic global tests including 50FC, 50RC. All local performance of seat investigated in local tests have the contrast in the global tests. E.g., HSST inspects whether the headrest can provide effective support when the heads of a passengers moves back forward while SBST is to investigate the support of backrest frame when passengers lean back. Videlicet, local static test quantitatively examines the specific performance indicators of a seat. Therefore, optimization parts are introduced into the global dynamic test with the maximum strain index, then using OLHS to carry out the discrete material and continuous thickness DoEs according to the part optimized grades obtained by GFLS.
- Specific test parts: OLHS is used to carry out DoEs according to the optimized grade "5" in the corresponding specific test, then import qualified design scheme with minimum total mass into the reconstruction model for verification.

V. OPTIMIZATION PROCESS

As shown in FIGURE 9, the SFMOO is divided into three phases: preprocessing phase, optimizing phase and reconstruction phase.

A. PREPROCESSING PHASE

The first step of SFMOO is the single-objective preprocessing of strong part, weak part and specific test working part. The purpose of the preprocessing phase is for making the seat frame meet the regulation requirements quickly, the single-objective optimization can also effectively reduce the design variables so that the sample points can get better filling with relatively less amounts. According to FIGURE 1, after determining the optimized attributes of a single part, the components that need preprocessing and the corresponding optimization tests are shown in Table 3. Meanwhile, the Equation 20 determines the number of sample points, then 10 and 15 points are exported to 50FC and 50RC respectively for preprocessing.

Besides, just one design variable need be optimized in HSST, and the DoE is not required, therefore 5 sample points are actively set. After preprocess, strong and weak parts will be imported into the "optimization part" for further optimization.

Preprocessing is a single-objective optimization, and the selection rule of optimal scheme is the minimum total mass while meeting the performance requirements of all tests. Optimal qualified design scheme will be imported into dynamic global tests for design verification. From the computation result after importing the preprocess optimal solution, the strain indices of all frame parts do not exceed the design thresholds and meet the requirements of all global tests.

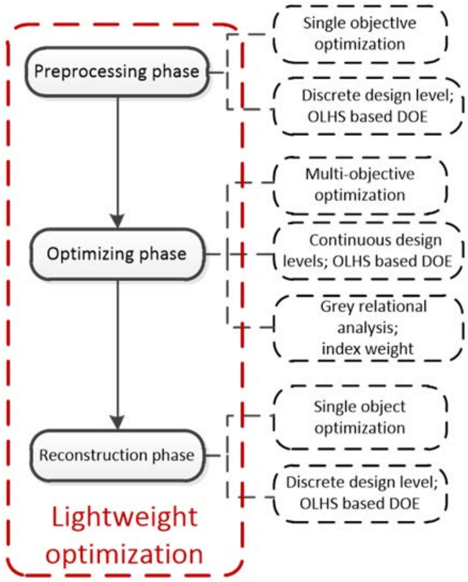

FIGURE 9. Flowchart of car seat frame optimization process.

TABLE 3. Parts need preprocessing and corresponding optimization safety tests.

Test	Optimization part	Optimized attribute	Optimization level
HSST	P1	specific test	
50FC	P13, P15, P16	strength	50%~90%, (5 levels)
50RC	P2, P3, P4, P7	strength	

B. PREPROCESSING PHASE

FIGURE 10 shows energy absorption of the same part in different global dynamic tests, in the following study, normal optimization parts are imported to the global dynamic test with higher energy absorption for further study.

Based on the deformation of parts in dynamic tests, GRC of energy absorption and mass for each part in corresponding test are acquire by calculation, and then they will be imported into GFLS along with relevant strain index. Furthermore, different from the defined eight optimized grades, specific optimized grade output by the GFLS is not an integer, so the following definition is added:

If the GFLS output of the ith part is $A.B$, then thickness range of the ith part is $[T_i \times (L_{Low_A} - B), T_i \times (L_{Up_A} - B)]$, and the material selected range is same as the roundness grade of $A.B$.

Where, T_i is the plate thickness before conducting DoE, $A.B$ is the calculated output optimized grade, L_{Low_A} is lower design bounds of optimized grade A, L_{Up_A} is upper design

TABLE 4. Output information of GFLS of optimization parts.

No.	Calculated Grade	Range of DoE (%)	Thickness (mm)	Material	Optimization test
P2	2.43	65.7-125.7	0.8-1.3	2-8	50RC
P3	2.44	65.6-125.7	0.6-1	5-11	50RC
P4	1.38	7.2-136.2	0.7-1	6-12	50RC
P7	2.6	64-124	1.6-2.9	5-11	50RC
P8	2.9	61-121	1.9-3.6	5-11	50RC
P9	2.57	64.3-124.3	1.2-2.2	5-11	50RC
P10	3.02	59.8-119.8	1.1-2.1	5-11	50FC
P11	2.32	66.8-126.8	2.1-3.8	4-10	50RC
P12	2.53	64.7-124.7	2.0-3.7	3-9	50FC
P13	1.5	75-135	1.6-2.7	4-10	50FC
P14	2.17	68.3-128.3	2.1-3.8	4-10	50FC
P15	2.93	60.7-120.7	1.9-3.6	15	50RC
P16	0.997	80.03-140.03	1.3-2.1	5-11	50RC
P17	2.53	64.7-124.7	0.6-0.9	4-10	50RC
P18	2.71	62.9-122.9	1.1-1.9	2-8	50RC
P19	3.12	58.7-118.7	0.5-0.9	1	50FC
P20	2.57	64.3-124.3	0.8-1.4	4-10	50FC

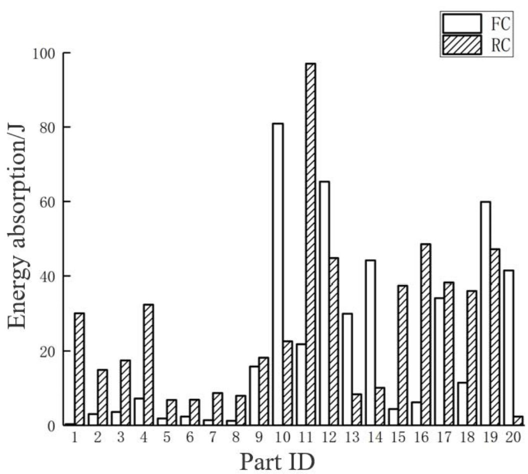

FIGURE 10. Verified energy absorption of each part from final preprocess model.

bounds of optimized grade A, A is the integer of $A.B$, B is the decimal place of $A.B$.

The calculated results of optimized grade for all components to be optimized in global safety tests are shown in Table 4.

Hence, the P10, P12, P13, P14, P19 and P20 are exported to 50FC for further optimization while P2, P3, P4, P7, P8, P9, P11, P15, P16, P17 and P18 are exported to 50RC for further optimization. Meanwhile, P1, P5 and P6 will not be lightweight optimized since specific test part P1 has been optimized in HSST and the strain indices of P5, P6 have reached 0.8 when preprocessing in SBST, namely, P5 and P6 are reasonably designed parts. Then, 36 and 121 sample points are set to 50FC and 50RC respectively for calculation according to the equation 20.

The study of SFMOO take lightweight, passenger comfort and safety performance into account. In this paper, lightweight targets include total mass and total cost, the comfort performance target is displacement of the point ''H'' inside the 50-percentile male dummy and the safety performance target is determined by optimization test. In 50FC, the adaptive performance target is Z- displacement of point A while the adaptive performance target in 50RC is the maximum change in backrest angle Db. The optimal tradeoff of 50FC and 50RC sequences can be easily obtained by using GRA.

On the anther hand, the research aim of this paper is to optimize the seat lightweight on the basis of ensuring the safety performance of the parts. Therefore, total mass and total cost are more important than comfort performance target and adaptive safety performance target. The unified weight of total mass, total cost, comfort performance target and adaptive safety performance target are 0.3, 0.3, 0.2, 0.2. Through Equation 14, the GRGs of each scheme can be calculated after GRCs and weights has been obtained. The scheme with biggest GRG is the optimal compromise in all example points. Table 5, Table 6 show the GRC, GRG in 50FC and 50RC after deleting waste points. Through comparison, the optimal compromise of 50FC is the example point 2, and the optimal compromise of 50RC is the example point 109.

C. RECONSTRUCTION PHASE

A new seat frame is reconstructed from optimized specific test parts, reasonably designed parts along with optimal

TABLE 5. GRCs and GRGs of partial sample points in 50FC.

NO.	Grey Relational Coefficient				GRG	Rank of GRG
	Displacement_*H*	Displacement_*A*	MASS	COST		
1	0.557666	0.506248	0.457768	0.460641	0.488305	28
2	0.333333	0.333333	1	1	0.733333	1
4	0.546032	0.52736	0.634913	0.601095	0.585481	14
5	0.471787	0.465201	0.493977	0.504099	0.48682	30
7	0.873096	1	0.507932	0.454188	0.663255	6
9	0.482952	0.538214	0.815862	0.83109	0.698319	3
…	…	…	…	…	…	…
33	0.564199	0.528609	0.687503	0.667801	0.625153	10
34	0.445102	0.446941	0.70948	0.692265	0.598932	12
35	0.726614	0.793536	0.388801	0.388844	0.537323	20
36	0.489829	0.445427	0.542066	0.544572	0.513043	25

TABLE 6. GRCs and GRGs of partial sample points in 50RC.

NO.	Grey Relational Coefficient				GRG	Rank of GRG
	Displacement_*H*	D_b	MASS	COST		
4	0.477319102	0.448145161	0.379759715	0.381427	0.413449	65
5	0.4586727	0.695842725	0.393352913	0.399964	0.468898	43
6	0.453880597	0.409204713	0.367752956	0.380336	0.397044	67
8	0.443100685	0.365015765	0.474233475	0.523631	0.460983	49
10	0.447469099	0.478639104	0.340278933	0.365357	0.396912	68
12	0.435548553	0.66992164	0.46550637	0.464545	0.50011	25
…	…	…	…	…	…	…
13	0.457844023	0.785552728	0.341597271	0.363376	0.460171	51
109	0.396479791	0.517700764	1	1	0.782836	1
120	0.431837546	0.628051537	0.41083409	0.411424	0.458655	53
121	0.436988073	0.667507508	0.40553732	0.424584	0.469936	40

compromises in 50FC and 50RC. It is conceivable that the reconstructed seat will most likely contain weak or strong parts due to the excessively weakened or conservatively structured design, so the weak and strong parts should be optimized again to ensure the necessary stiffness of the reconstruction seat frame. On the basis of the simulation results of reconstructed model in all tests, the P15 and P16 are considered as strong parts which have the largest strain index in SBST. Moreover, P11 broken in SBST, is a weak part.

Specific optimization process stipulates that P15 and P16 are weakened under the optimized grade "5". Updating the optimal P15 and P16 scheme to the seat model and recalculate. Afterwards, strengthening P11 as requested of optimized grade "-1". Since the equation 20, the number of sample points for weakening P15 and P16 is 10, the amount of sample points for strengthening P11 is 5.

TABLE 7. The fitting accuracy from RBF.

	Cost	Mass	Displacement_H	Displacement_A
R^2	0.988	0.994	0.099	0
ME	0.083	0.065	0.429	0.518
RMSE	0.019	0.013	0.189	0.222

VI. RESULT AND DISCUSSION

The design information of the seat frame in final optimum design scheme shows that total mass and total material cost of the seat frame before the proposed optimization are 8.0kg and ¥40.8 respectively. Meanwhile, the total mass and total material cost of the seat frame after the proposed optimization are reduced to 5.7kg (-28.5%) and ¥27.6 (-32.4%). At the same time, the seat frame still meets the performance requirements of various safety tests. Besides, it is necessary to further

TABLE 8. Detailed mass, cost comparisons between the original design, the optimum compromise design from the method in this paper and the optimum design from the comparison MW.

No.	origin design		optimum design from the proposed method		optimum design from the comparison method	
	MASS	COST	MASS	COST	MASS	COST
P1	0.430	2.052	0.301	1.436	0.301	1.536
P2	0.591	3.015	0.355	1.593	0.552	2.985
P3	0.548	2.794	0.365	1.976	0.457	2.305
P4	0.548	2.794	0.320	1.729	0.411	2.223
P5	0.181	0.914	0.181	0.914	0.199	1.025
P6	0.181	0.914	0.181	0.914	0.127	0.655
P7	0.300	1.551	0.200	1.020	0.350	1.785
P8	0.300	1.551	0.250	1.293	0.280	1.442
P9	0.559	2.887	0.403	2.182	0.434	2.246
P10	0.559	2.888	0.372	2.316	0.559	2.821
P11	0.562	2.839	0.450	2.366	0.506	2.580
P12	0.490	2.476	0.458	0.451	0.523	2.580
P13	0.134	0.677	0.089	0.714	0.143	2.668
P14	0.140	0.707	0.140	0.714	0.112	0.739
P15	0.234	2.221	0.051	0.481	0.226	2.147
P16	0.149	0.753	0.065	0.326	0.114	0.577
P17	0.334	1.702	0.250	1.264	0.417	2.127
P18	0.455	2.341	0.341	1.756	0.369	1.909
P19	0.931	3.983	0.698	2.987	0.814	3.485
P20	0.343	1.748	0.228	1.165	0.257	1.324
Sum	7.967	40.805	5.698	27.597	7.151	39.159

illustrate the advantages of the proposed seat frame hierarchical optimization method employing GFLS for adaptive DoEs. Hence, taking all seat frame parts as the objects to be optimized and setting 50FC as the verification safety test. 7 discrete material parameters and 70%∼130% continuous thickness variables are introduced as range of DoE, the sample size is set to 200 through OLHS. Model of surrogate model and multi-criteria decision making are both used.

A. SURROGATE MODEL EMPLOYING RBF

The high-precision surrogate model is the most important guarantee of the reliable results when employing AOW. The commonly adopted fitting methods in engineering application includes response surface methodology (RSM), Kriging model and radial basis function (RBF) and so on [32]. RBF is fitted with the highest precision although the it still can not meet the requirements of subsequent optimization. FIGURE 11 shows the fitting process and Table 7 shows the calculation results of fitting accuracy from RBF. R^2, ME and RMSE are used to calculate the fitting accuracy. R^2 is the deterministic coefficient, the larger R^2 shows the better the fitting accuracy. ME means the maximum error, RMSE means the root mean square error, the smaller ME and RMSE show the better the fitting accuracy. Expressly, the RMSE and R^2 reflect the overall accuracy of the surrogate model while the ME represents the local accuracy

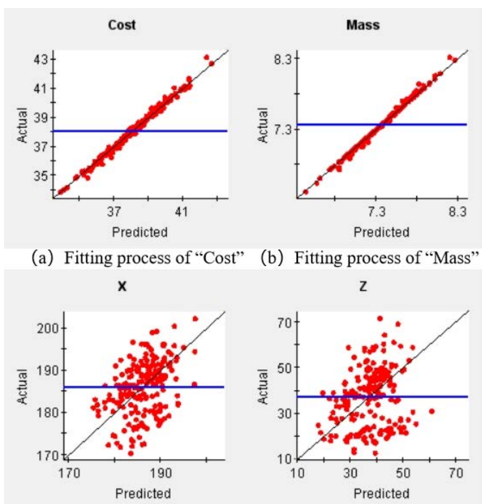

(a) Fitting process of "Cost" (b) Fitting process of "Mass"
(c) Fitting process of "*H* displacement" (d) Fitting process of "*A* displacement"

FIGURE 11. The fitting process of RBF.

of the model. It can be found from the Table 7, since the displacement are nonlinear variables, the fitting accuracy of the displacement of point H and A are unqualified so that AOW can not obtain reliable results in the case of a few sample points.Therefore, the multi-objective optimization of the auto seat frame cannot be solved through AOW when adopting few amount of sample points.

B. MULTI-OBJECTIVE DECISION-MAKING WITHOUT ADAPTIVE DOE AND HIERARCHICAL OPTIMIZATION

Based on the 200 sample points from OLHS in 50FC, GRA and coefficient of variation method which have been proven an effective way by Shan [25] for the multi-objective optimization of the auto seat frame is adopted to obtain the optimal solution for the companion. The weights given by coefficient of variation method are 0.209,0.261,0.260,0.270 respectively. After calculation and summary, total frame mass and material cost of the optimal compromise acquired through the contrast method are 7.2kg and ￥37.1, which reduced by 10.2% and 9.0% compared to the original design. Detailed mass, cost of a single component from the original design, the optimum design obtained by proposed method in this paper and the optimum design obtained by GRA and coefficient of variation method are listed in Table 8.

VII. CONCLUSION AND FUTURE RESEARCHES

In this paper, all seat frame parts are taken as the optimization objects, and a set of hierarchical seat lightweight optimization methods are proposed. For the purpose of reducing the sample size for design of experiments (DoEs), the seat frame multi-objective optimization (SFMOO) is divided into three phases. Meanwhile, employing the grey fuzzy logic system (GFLS) for determining optimized grade of frame parts to avoid the error caused by manual selection or same design ranges. Subsequently, adopting optimized Latin hypercube sampling method (OLHS) for design of experiments. Totally, 197 sample points are used, grey relational analysis (GRA) is used to determine the optimal compromise scheme in example points. According to relevant research results and comparison, following conclusions can be drawn:

(1) The proposed method in this paper decreases the total mass and material cost by 2.3kg (28.5%) and ￥13.8 (32.4%) respectively while all frame parts are optimized and a small sample size.

(2) For the purpose of determining the specific optimized grades of normal optimization parts, grey fuzzy logic system (GFLS) and optimized Latin hypercube sampling (OLHS) are combined to adaptively construct design of experiments (DoEs). This innovation can effectively trim the design space and improve the filling ability of the sample points.

(3) Under the condition that a small sample sizes are given, the conventional AOW can not build the surrogate proxy model while the MW only obtain limited optimization effect. Meanwhile, it can be intuitively found that the optimal compromise of the conventional MW method (10.2% mass reduction and 9.0% cost reduction)is worse than that (28.5% mass reduction and 32.4% cost reduction) of the method proposed in this paper. At the same time, the safety performance of passenger car seat is guaranteed and meets the all-applied tests requirements after the seat frame hierarchical multi-objective optimization.

(4) The proposed method in this paper is suitable for high dimensional auto parts multi-objective optimization with the following characteristics: multiple design variables, multiple design levels, multiple safety tests and long calculation time.

(5) Although the validity of proposed method is verified through comparison, it must be said that this paper applies the unified weight. In other words, we determine the importance of the four optimization targets through experience. Manually defined fuzzy rules are generated from the engineer experience. Fuzzy rules can also reflect the importance of all targets in the mind of engineers. Refining the fuzzy rules is a solution to replace the unified weight.

(6) GFLS makes decisions on the basis of engineer experience deliberately while GRA processes data only based on the internal relationship of initial sequences. Therefore,we will implement fuzzy decision-making to improve the integration of GFLS in further researches. This will further improve the usability of this method.

REFERENCES

[1] J. W. McAuley, "Global sustainability and key needs in future automotive design," *Environ. Sci. Technol.*, vol. 37, no. 23, pp. 5414–5416, Dec. 2003.

[2] A. R. Yildiz, N. Pholdee, and S. Bureerat, "Hybrid real-code population-based incremental learning and differential evolution for many-objective optimisation of an automotive floor-frame," *Int. J. Vehicle Des.*, vol. 73, nos. 1–3, pp. 20–53, Mar. 2017.

[3] S. Yin, H. Chen, Y. Wu, Y. Li, and J. Xu, "Introducing composite lattice core sandwich structure as an alternative proposal for engine hood," *Composite Struct.*, vol. 201, pp. 131–140, Oct. 2018.

[4] T. Wang, R. Dong, S. Zhang, and D. Qin, "Research on lightweight design of automobile collision safety structure based on multiple materials," *J. Phys., Conf. Ser.*, vol. 1670, no. 1, Nov. 2020, Art. no. 012004.

[5] D. Wang, S. Zhang, C. Wang, and C. Zhang, "Structure-material-performance integration lightweight optimisation design for frontal bumper system," *Int. J. Crashworthiness*, vol. 23, no. 3, pp. 311–327, 2017.

[6] J. Zhang, J. Chen, Z. Li, M. Ji, and T. Sang, "Optimisation design of CFRP passenger car seat backplane based on impact characteristics," *Int. J. Crashworthiness*, vol. 26, no. 4, pp. 355–367, 2020.

[7] F. Henning, L. Kärger, D. Dörr, F. J. Schirmaier, J. Seuffert, and A. Bernath, "Fast processing and continuous simulation of automotive structural composite components," *Compos. Sci. Technol.*, vol. 171, pp. 261–279, Feb. 2019.

[8] N. M. Ishak, D. Sivakumar, and M. R. Mansor, "The application of TRIZ on natural fibre metal laminate to reduce the weight of the car front hood," *J. Brazilian Soc. Mech. Sci. Eng.*, vol. 40, no. 2, p. 105, Feb. 2018.

[9] L. Duan, H. Jiang, A. Cheng, H. Xue, and G. Geng, "Multi-objective reliability-based design optimization for the VRB-VCS FLB under front-impact collision," *Struct. Multidisciplinary Optim.*, vol. 59, no. 5, pp. 1835–1851, May 2019.

[10] L. Duan, H. Jiang, G. Geng, X. Zhang, and Z. Li, "Parametric modeling and multiobjective crashworthiness design optimization of a new front longitudinal beam," *Struct. Multidisciplinary Optim.*, vol. 59, no. 5, pp. 1789–1812, May 2019.

[11] L. Duan, X. Liu, W. Xu, D. Xu, L. Shi, and H. Jiang, "Thickness-based subdomian hybrid cellular automata algorithm for lightweight design of BIW under side collision," *Appl. Math. Model.*, vol. 102, pp. 170–193, Feb. 2022.

[12] L. Duan, N.-C. Xiao, Z. Hu, G. Li, and A. Cheng, ''An efficient lightweight design strategy for body-in-white based on implicit parameterization technique,'' *Struct. Multidisciplinary Optim.*, vol. 55, no. 5, pp. 1927–1943, May 2017.

[13] G. Sun, D. Tan, X. Lv, X. Yan, Q. Li, and X. Huang, ''Multi-objective topology optimization of a vehicle door using multiple material tailor-welded blank (TWB) technology,'' *Adv. Eng. Softw.*, vol. 124, pp. 1–9, Oct. 2018.

[14] G. G. Fossati, L. F. F. Miguel, and W. J. P. Casas, ''Multi-objective optimization of the suspension system parameters of a full vehicle model,'' *Optim. Eng.*, vol. 20, no. 1, pp. 151–177, Mar. 2019.

[15] Q. Gao, L. Wang, Y. Wang, and C. Wang, ''Crushing analysis and multiobjective crashworthiness optimization of foam-filled ellipse tubes under oblique impact loading,'' *Thin-Walled Struct.*, vol. 100, pp. 105–112, Mar. 2016.

[16] H.-S. Kim, Y.-S. Lee, S.-M. Yang, and H. Y. Kang, ''Structural analysis on variable characteristics of automotive seat frame by FEA,'' *Int. J. Precis. Eng. Manuf.-Green Technol.*, vol. 3, no. 1, pp. 75–79, Jan. 2016.

[17] L. Hongling, D. Yude, C. Changliang, and C. Chao, ''Combined with finite element analysis of car seat safety performance improvement,'' *J. Mech. Sci. Technol.*, vol. 35, no. 1, pp. 79–89, Jan. 2021.

[18] A. Siefert, S. Pankoke, and H.-P. Wölfel, ''Virtual optimisation of car passenger seats: Simulation of static and dynamic effects on drivers' seating comfort,'' *Int. J. Ind. Ergonom.*, vol. 38, nos. 5–6, pp. 410–424, May 2008.

[19] K. Soorya Prakash, P. M. Gopal, and S. Karthik, ''Multi-objective optimization using Taguchi based grey relational analysis in turning of rock dust reinforced aluminum MMC,'' *Measurement*, vol. 157, Jun. 2020, Art. no. 107664.

[20] D. Wang and K. Cai, ''Optimizing the static-dynamic performance of the body-in-white using a modified non-dominated sorting genetic algorithm coupled with grey relational analysis,'' *Eng. Optim.*, vol. 50, no. 4, pp. 615–633, 2017.

[21] F. Xiong, D. Wang, S. Zhang, K. Cai, S. Wang, and F. Lu, ''Lightweight optimization of the side structure of automobile body using combined grey relational and principal component analysis,'' *Struct. Multidisciplinary Optim.*, vol. 57, no. 1, pp. 441–461, Jan. 2018.

[22] Y. Pu, F. Ma, L. Han, and G. Wang, ''Material selection of green design processes for car body via considering environment property,'' *Math. Problems Eng.*, vol. 2020, pp. 1–8, Mar. 2020.

[23] F. Xiong, X. Zou, Z. Zhang, and X. Shi, ''A systematic approach for multi-objective lightweight and stiffness optimization of a car body,'' *Struct. Multidisciplinary Optim.*, vol. 62, no. 6, pp. 3229–3248, Dec. 2020.

[24] K. Cai and D. Wang, ''Optimizing the design of automotive S-rail using grey relational analysis coupled with grey entropy measurement to improve crashworthiness,'' *Structural Multidisciplinary Optim.*, vol. 56, no. 6, pp. 1539–1553, Dec. 2017.

[25] Z. Shan, J. Long, P. Yu, L. Shao, and Y. Liao, ''Lightweight optimization of passenger car seat frame based on grey relational analysis and optimized coefficient of variation,'' *Struct. Multidisciplinary Optim.*, vol. 62, no. 6, pp. 3429–3455, Dec. 2020.

[26] S.-I. Moon, D.-S. Shin, E.-S. Jeon, and S.-M. Cha, ''Discrete material and thickness optimization of pop-up seat frame in static condition,'' *Int. J. Mech. Eng. Technol.*, vol. 11, no. 1, pp. 23–39, Jan. 2020.

[27] J. Zhang, Z. Li, Q. Fang, and C. Chen, ''Topological optimisation design of passenger car seat backrest frame based on multiple-loading conditions,'' *Int. J. Crashworthiness*, vol. 25, no. 5, pp. 1–10, 2019.

[28] J. Zhang, Z. Li, T. Sang, and M. Ji, ''Structure design of LFT passenger car seat structure based on topology optimisation,'' *Int. J. Crashworthiness*, vol. 26, no. 6, pp. 617–627, 2020.

[29] K. Liu, ''Post-earthquake medical evacuation system design based on hierarchical multi-objective optimization model: An earthquake case study,'' *Int. J. Disaster Risk Reduction*, vol. 51, Dec. 2020, Art. no. 101785.

[30] L. Sun, Q. Zhou, B. Jia, W. Tan, and L. I. Hangxu, ''Effective control allocation using hierarchical multi-objective optimization for multi-phase flight,'' *Chin. J. Aeronaut.*, vol. 33, no. 7, p. 12, 2020.

[31] K. Ramakrishnan, G. Mastinu, and M. Gobbi, ''Multidisciplinary design of electric vehicles based on hierarchical multi-objective optimization,'' *J. Mech. Des.*, vol. 141, no. 9, Sep. 2019, Art. no. 091404.

[32] J. Long, Y. Liao, and P. Yu, ''Multi-response weighted adaptive sampling approach based on hybrid surrogate model,'' *IEEE Access*, vol. 9, pp. 45441–45453, 2021.

[33] W. Hou, X. Xu, X. Han, H. Wang, and L. Tong, ''Multi-objective and multi-constraint design optimization for hat-shaped composite T-joints in automobiles,'' *Thin-Walled Struct.*, vol. 143, Oct. 2019, Art. no. 106232.

[34] A. A. Pasha Zanoosi, M. Mallakzadeh, and R. Kalantarinejad, ''Optimal frame geometry of spacecraft seat based on multi-body dynamics modelling,'' *Acta Astronautica*, vol. 115, pp. 58–70, Oct. 2015.

[35] L. Hou, H. Zhang, Y. Peng, S. Wang, S. Yao, Z. Li, and G. Deng, ''An integrated multi-objective optimization method with application to train crashworthiness design,'' *Struct. Multidisciplinary Optim.*, vol. 63, no. 3, pp. 1513–1532, Mar. 2021.

[36] X. Cui, S. Wang, and S. J. Hu, ''A method for optimal design of automotive body assembly using multi-material construction,'' *Mater. Des.*, vol. 29, no. 2, pp. 381–387, 2008.

[37] F. Xiong, D. Wang, and S. Yin, ''Optimization analysis of novel foam-filled elliptical columns under multiple oblique impact loading,'' *Mater. Des.*, vol. 156, pp. 198–214, Oct. 2018.

[38] J. L. Deng, ''Introduction to Grey system theory,'' *J. Grey Syst.*, vol. 1, no. 1, pp. 1–24, 1989.

[39] D. Ju-Long, ''Control problems of grey systems,'' *Syst. Control Lett.*, vol. 1, no. 5, pp. 288–294, 1982.

[40] Y. Kuo, T. Yang, and G.-W. Huang, ''The use of grey relational analysis in solving multiple attribute decision-making problems,'' *Comput. Ind. Eng.*, vol. 55, no. 1, pp. 80–93, Aug. 2008.

[41] E. H. Mamdani, ''Application of fuzzy algorithms for control of simple dynamic plant,'' *Proc. Inst. Electr. Eng.*, vol. 121, no. 12, pp. 1585–1588, 1974.

[42] L. A. Zadeh, ''Fuzzy algorithms,'' *Inf. Control*, vol. 12, no. 2, pp. 94–102, 1968.

[43] L. A. Zadeh, ''Outline of a new approach to the analysis of complex systems and decision processes,'' *IEEE Trans. Syst., Man, Cybern.*, vols. SMC-3, no. 1, pp. 28–44, Jan. 1973.

[44] A.-T. Nguyen, T. Taniguchi, L. Eciolaza, V. Campos, R. Palhares, and M. Sugeno, ''Fuzzy control systems: Past, present and future,'' *IEEE Comput. Intell. Mag.*, vol. 14, no. 1, pp. 56–68, Feb. 2019.

[45] W. R. Mendes, F. M. U. Araújo, R. Dutta, and D. M. Heeren, ''Fuzzy control system for variable rate irrigation using remote sensing,'' *Expert Syst. Appl.*, vol. 124, pp. 13–24, Jun. 2019.

[46] L. Fang, S. Ding, J. H. Park, and L. Ma, ''Adaptive fuzzy control for non-triangular stochastic high-order nonlinear systems subject to asymmetric output constraints,'' *IEEE Trans. Cybern.*, vol. 52, no. 2, pp. 1280–1291, Feb. 2022.

[47] W. Sun, S.-F. Su, Y. Wu, and J. Xia, ''Novel adaptive fuzzy control for output constrained stochastic nonstrict feedback nonlinear systems,'' *IEEE Trans. Fuzzy Syst.*, vol. 29, no. 5, pp. 1188–1197, May 2021.

[48] S. A. Bhat, A. Singh, and A. A. and Qudaimi, ''A new Pythagorean fuzzy analytic hierarchy process based on interval-valued Pythagorean fuzzy numbers,'' *Fuzzy Optim. Model. J.*, vol. 2, no. 4, pp. 38–51, 2021.

[49] A. Ebrahimnejad, M. Tavana, and V. Charles, ''Analytics under uncertainty: A novel method for solving linear programming problems with trapezoidal fuzzy variables,'' *Soft Comput.*, vol. 26, pp. 327–347, Nov. 2021.

[50] A. Sorourkhah and S. A. Edalatpanah, ''Considering the criteria interdependency in the matrix approach to robustness analysis with applying fuzzy ANP,'' *Fuzzy Optim. Model. J.*, vol. 2, no. 2, pp. 22–33, 2021.

[51] A. A. Sori, A. Ebrahimnejad, H. Motameni, and J. L. Verdegay, ''Fuzzy constrained shortest path problem for location-based online services,'' *Int. J. Uncertainty, Fuzziness Knowl.-Based Syst.*, vol. 29, no. 2, pp. 231–248, Apr. 2021.

[52] M. Bagheri, A. Ebrahimnejad, S. Razavyan, F. H. Lotfi, and N. Malekmohammadi, ''Fuzzy arithmetic DEA approach for fuzzy multi-objective transportation problem,'' *Oper. Res.*, vol. 22, pp. 1479–1509, Aug. 2020.

[53] A. A. Sori, A. Ebrahimnejad, and H. Motameni, ''Elite artificial bees' colony algorithm to solve robot's fuzzy constrained routing problem,'' *Comput. Intell.*, vol. 36, no. 2, pp. 659–681, May 2020.

[54] W. Yao, K. Cai, and Y. Xu, ''Optimizing the beam-like structure of a vehicle body using the grey-fuzzy-Taguchi method,'' *Eng. Optim.*, no. 8, pp. 1–22, 2020.

[55] Q. P. Tran, T. Le, and S. C. Huang, ''Multi-objective optimization of carbon fiber-reinforced polymer drilling process based on grey fuzzy reasoning grade analysis,'' *Int. J. Adv. Manuf. Technol.*, vol. 115, pp. 503–513, May 2021.

[56] T. Takagi and M. Sugeno, ''Fuzzy identification of systems and its applications to modeling and control,'' *Readings Fuzzy Sets Intell. Syst.*, vol. 15, no. 1, pp. 387–403, 1993.

[57] J.-S. R. Jang, "ANFIS: Adaptive-network-based fuzzy inference system," *IEEE Trans. Syst., Man, Cybern.*, vol. 23, no. 3, pp. 665–685, May 1993.
[58] B. M. Keneni, D. Kaur, A. Al Bataineh, V. K. Devabhaktuni, A. Y. Javaid, J. D. Zaientz, and R. P. Marinier, "Evolving rule-based explainable artificial intelligence for unmanned aerial vehicles," *IEEE Access*, vol. 7, pp. 17001–17016, 2019.
[59] V. S. Araújo, A. Guimarães, P. de Campos Souza, T. S. Rezende, and V. S. Araújo, "Using resistin, glucose, age and BMI and pruning fuzzy neural network for the construction of expert systems in the prediction of breast cancer," *Mach. Learn. Knowl. Extraction*, vol. 1, no. 1, pp. 466–482, Feb. 2019.
[60] B. Wu, T. L. Yip, X. Yan, and C. G. Soares, "Fuzzy logic based approach for ship-bridge collision alert system," *Ocean Eng.*, vol. 187, Sep. 2019, Art. no. 106152.
[61] X. L. Liu, Y. W. Chen, X. R. Jing, and Y. G. Chen, "Optimized Latin hypercube sampling method and its application," *J. Nat. Univ. Defense Technol.*, vol. 33, no. 5, pp. 73–77, 2011.
[62] F. A. C. Viana, G. Venter, and V. Balabanov, "An algorithm for fast optimal Latin hypercube design of experiments," *Int. J. Numer. Methods Eng.*, vol. 82, no. 2, pp. 135–156, Apr. 2010.
[63] P. Feng, "Ensemble of surrogate models for lightweight design of autobody structure," Ph.D. dissertation, School Mech. Power Eng., Shanghai Jiaotong Univ., Shanghai, China, 2011.

WEI WANG was born in 1996. He is currently pursuing the degree with the School of Mechanical and Electrical Engineering, Wenzhou University. His research interests include lightweight design of auto parts, fuzzy control, and multi-objective optimization.

XIAOJUN LAN is currently the Director of the Technology Research and Development Department, Wenzhou Dongqi Auto Parts Manufacturing Company Ltd. His research interests include the products development of automotive brake master cylinder, brake wheel cylinder, cooling water pump, and other auto products.

JIANGQI LONG is currently a Professor with the College of Mechanical and Electrical Engineering, Wenzhou University. His research interests include performance analysis and lightweight design theory of car body structure, and structural design and multidisciplinary optimization of auto parts.